

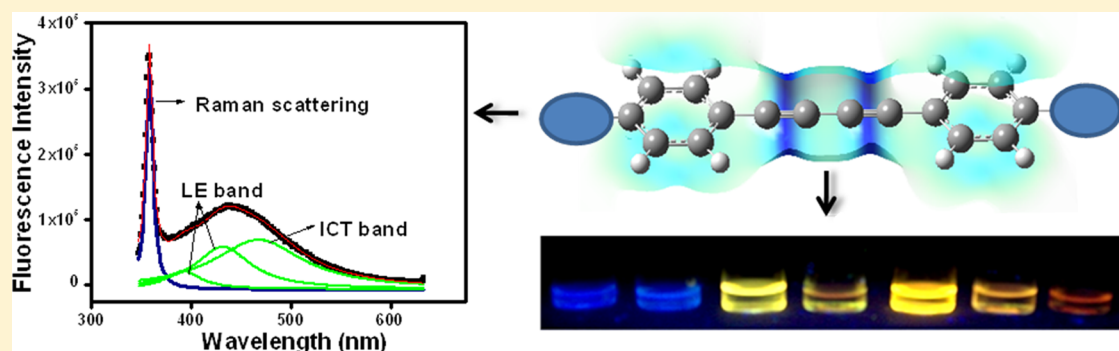
Deciphering the Photophysical Role of Conjugated Diyne in Butadiynyl Fluorophores: Synthesis, Photophysical and Theoretical Study

Avik Kumar Pati,[†] Monalisa Mohapatra,[†] Pokhraj Ghosh,[†] Santosh J. Gharpure,^{*,†,‡} and Ashok K. Mishra^{*,†}

[†]Department of Chemistry, Indian Institute of Technology Madras, Chennai 600036, Tamil Nadu, India

[‡]Department of Chemistry, Indian Institute of Technology Bombay, Powai, Mumbai 400076, India

S Supporting Information



ABSTRACT: The present work focuses on the current interest in diyne bridged chromophores necessitating a clearer understanding of the photophysics of such molecules. The significance of the diyne moiety in the photophysics has been investigated by synthesizing simple substituted diphenyl butadiynyl derivatives following a quick and efficient microwave assisted Eglinton coupling of terminal alkynes. Emission of the fluorophores is observed from the usual locally excited (LE) state and intramolecular charge transfer (ICT) state. Separation of pure ICT emission from pure LE emission has been carried out by Gaussian/Lorentzian curve fitting. The vibronic coupling in the local transitions appears to be confined to the normal mode involving the C–C triple bond stretching of the diyne moiety. This implies that the LE transition involves the diyne moiety, a conclusion supported by quantum chemical calculations. The resolved ICT emission follows double linear dependence on $E_T(30)$ solvent polarity scale. The important role of the diyne moiety in the photophysics of this class of molecules is clearly discernible in this study.

INTRODUCTION

Recent years have seen an upsurge in the development of novel organic fluorophores exhibiting intramolecular charge transfer (ICT) owing to their efficacious applications in field effect diodes,^{1,2} light emitting diodes,^{3,4} chemical sensors,^{5–7} and in many other photochemical and photobiological processes.^{8–10} Often these fluorophores are found to contain alkyne units in conjugation with different aromatic moieties. Thus the chemistry of triple bond attached fluorophores is very rich. Surprisingly, a deeper photochemical understanding of conjugated two triple bonds, that is, butadiyne moiety, remains scarce in the literature from a long time ago. Nevertheless, some efforts have been made in recent years.^{11–35} Bryce et al. have explored the photophysics of 2,5-diphenyl-1,3,4-oxadiazole (OXD) containing butadiynyl derivatives.^{13,14} Otera and Orita et al. have exploited the photochemistry of diphenylamino substituted phenylene-(poly)ethynylene derivatives.^{15,16} The photochemistry of a butadiyne conjugated pyrene dimer has been disclosed by Benniston et al.²² Very recently, a

structure–property relationship of butadiyne conjugated carbazole dimers has been described by Nakamura et al.³⁵ These studies notwithstanding, the photophysics of the butadiyne moiety itself is not completely unravelled. This is because most of these studies either include the butadiyne moiety attached to inherent fluorophores/bulkier aromatic groups or the butadiyne moiety is overloaded with extended alkyne conjugation, thereby masking the original photophysical contribution from the butadiyne part. Thus an understanding of the contribution of the butadiyne moiety to the photophysics of such molecular systems assumes importance. The diyne moiety has even found its applications in nanoscience,³⁶ molecular rotors,³⁷ liquid crystals,^{38–41} and antiviral activities⁴² providing an impetus for contemporary research. Intriguingly, the ubiquity of this moiety in several biologically active natural

Received: May 16, 2013

Revised: July 2, 2013

Published: July 3, 2013

Scheme 1. Retrosynthesis of Diyne 1

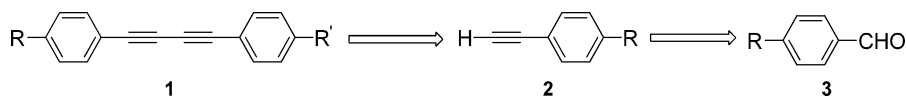
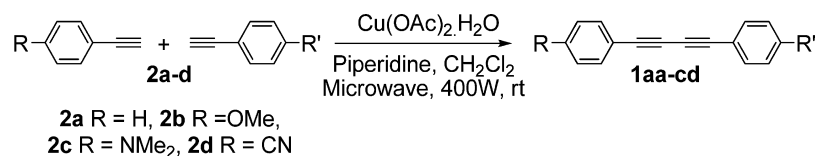


Table 1. Synthesis of Diyne Derivatives 1aa–cd



Entry	Alkyne	Time (min.)	Product	Yield ^a (%)
1.	R = R' = H	10		99
2.	R = R' = OMe	10		98
3.	R = R' = Me ₂ N	10		85
4.	R = H (5eq.), R' = OMe (1eq.)	15		75
5.	R = H (5eq.), R' = CN (1eq.)	15		66
6.	R = H (5eq.), R' = Me ₂ N (1eq.)	15		74
7.	R = Me ₂ N (1eq.), R' = OMe (5eq.)	15		78
8.	R = Me ₂ N (5eq.), R' = CN (1eq.)	15		73

^aIsolated yields of purified product.

products⁴³ attracts special attention to look at its fundamental photophysical properties.

At this juncture, we envisaged that the role of the diyne moiety in controlling photophysical behavior of a butadiynyl derivative could be properly investigated only when the aromatic moieties attached to the periphery of the diyne are as simple as phenyl ring such that they do not perturb the photophysical properties of core diyne moiety. Thus, simply substituted 1,3-diphenyl butadiynes could be fundamentally important representatives to study the effect of the diyne moiety in deciding photochemical behavior of a fluorophore. The objectives of this work are (1) to develop a synthetic root for the quick access of diynes, especially photophysically important hetero diynes despite synthetic challenges, (2) to study a detailed and systematic photophysical behavior of the derivatives in a series of solvents of different polarities, (3) to find a uniform model to understand the photophysical properties, and (4) to understand better the electronic structure of diynes through theoretical calculations.

RESULTS AND DISCUSSION

Synthesis. A number of methods for coupling reactions of terminal alkynes are documented in the literature. Among all of them, Glaser,⁴⁴ Eglinton,⁴⁵ Hay,^{46,47} Cadiot-Chodkiewicz^{48,49} and Sonogashira^{50,51} reactions are well-known.⁵² Recently, a fast, solvent free, microwave assisted heterogeneous homocoupling of terminal alkynes on alumina surface is reported.⁵³ The protocol was limited to only homocoupling in heterogeneous phase. Here, we wish to report a microwave assisted homogeneous Eglinton coupling of terminal alkynes for the quick access to both homo- and heterocoupling products. The retrosynthetic analysis for the synthesis of 1,3-diyne **1** is depicted in Scheme 1. Commercially available phenyl acetylene was directly used for reaction purposes, and the other alkynes were prepared from the corresponding aldehydes using literature reported procedures.^{54–56} With the requisite alkynes in hand, we turned our attention toward the synthesis of 1,3-diyne **1aa–cd** via microwave assisted Cu(II) catalyzed homogeneous Eglinton reaction of alkynes. Cu(OAc)₂ was used as salt, and piperidine was used as base.⁵⁷ To test the feasibility of the reaction, phenyl acetylene **2a** was first subjected to microwave assisted homogeneous homocoupling

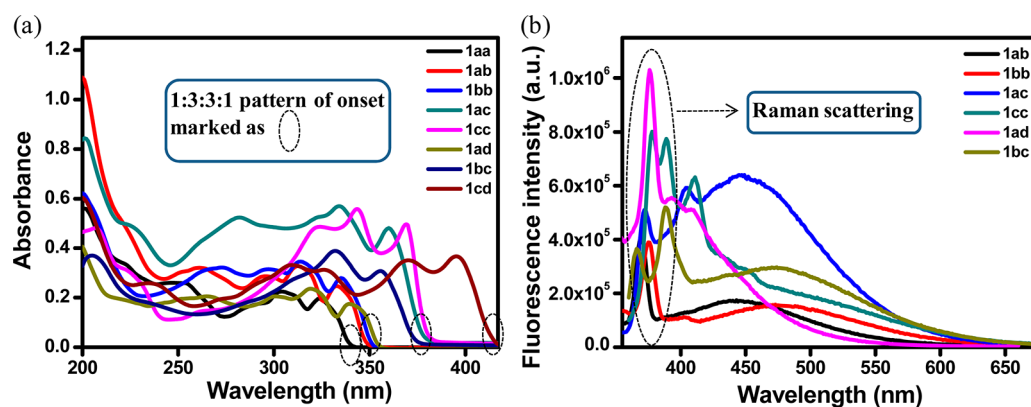


Figure 1. (a) Absorption spectra of 1aa–cd and (b) emission spectra of 1aa–bc in cyclohexane (10^{-5} M, $\lambda_{\text{ex}} = 335, 340, 330, 350, 340, 350$ nm for 1ab, 1bb, 1ac, 1cc, 1ad, 1bc, respectively).

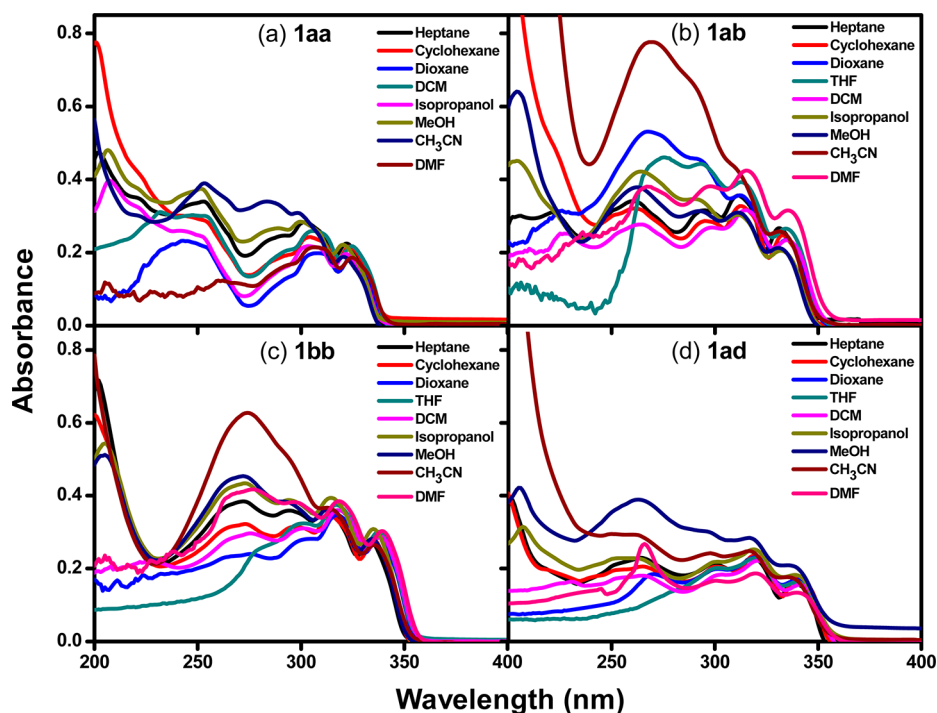


Figure 2. UV–vis spectra of (a) 1aa, (b) 1ab, (c) 1bb, and (d) 1ad in various solvents (10^{-5} M).

reaction to give the corresponding diyne **1aa** in excellent yield (Table 1, entry 1). The identity of the compound was ascertained from its spectral data. Encouraged by this result, various alkynes were subjected to homo- and heterocoupling reactions under the same reaction conditions, and various 1,3-diyne were obtained in good to excellent yields (Table 1, entry 2–8). The identities of the compounds were confirmed by NMR spectral analysis which was further confirmed by mass spectral analysis. Heterocoupling reaction was carried out using two different terminal alkynes in the ratio of 1:5. It is pertinent to mention that each hetero coupling reaction ended up with the formation of homocoupling products of the alkynes along with a major heterocoupling derivative. The required product was purified by extensive column chromatography to ascertain the absence of impurities. Each compound was finally filtered through silica column using HPLC grade hexane and recrystallized prior to photophysical studies.

Absorption and Emission Spectra in Cyclohexane. Cyclohexane being a nonpolar, noninteractive solvent, UV–vis

and emission spectra of all compounds were recorded in cyclohexane. A closer look at the onset of electronic absorption spectra reveals that eight molecules here under study can be divided into four groups as if the spectral features among the molecules are distributed over 1:3:3:1 pattern (Figure 1a). The onset of electronic absorption shifts bathochromically from parent molecule **1aa** to methoxy substituted derivatives **1ab**, **1bb** and nitrile substituted **1ad** to dimethyl amino substituted derivatives **1cc**, **1ac**, **1bc** to donor dimethyl amino and acceptor nitrile substituted derivative **1cd**. This gradual red shift indicates the presence of ICT through the butadiynyl moiety.

The parent chromophore **1aa** was found to be non fluorescent^{25,26} under our experimental conditions. Emission spectra of all other derivatives in cyclohexane were found to be structured with long band/tail extended to the longer wavelength (Figure 1b). Fluorescence intensity was found to be higher for dimethyl amino substituted derivatives while comparing with methoxy derivatives. Owing to the structural emission spectrum in non polar cyclohexane, we were keen to

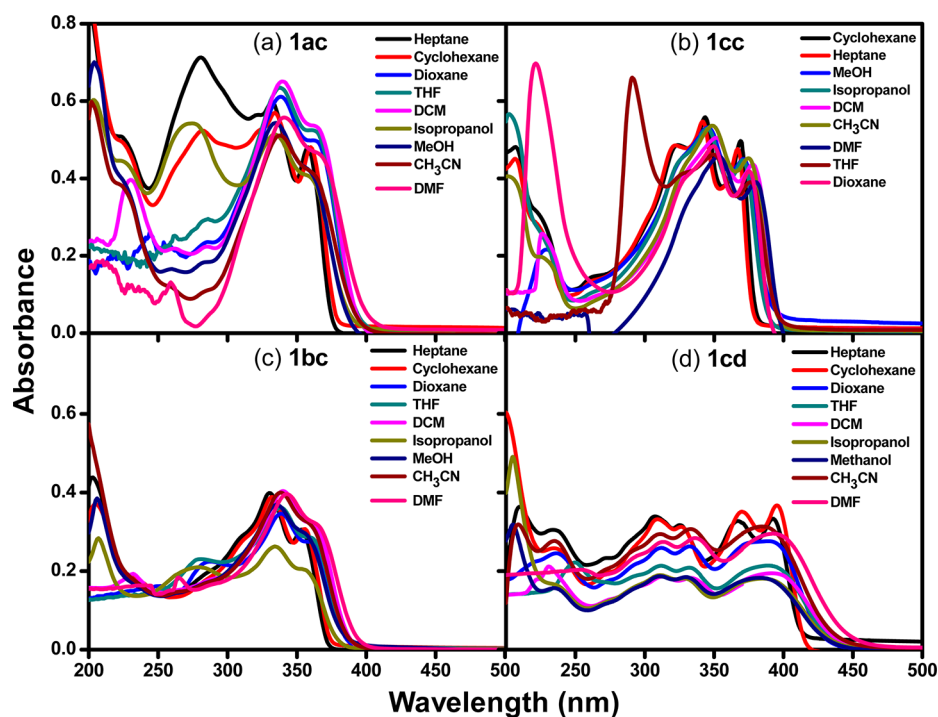


Figure 3. UV-vis spectra of (a) **1ac**, (b) **1cc**, (c) **1bc**, and (d) **1cd** in various solvents (10^{-5} M).

observe its effect in polar solvents. At this junction, we envisioned that a detailed solvatochromic investigation of UV-vis and emission spectra might reveal some important features of the butadiyne moiety.

Absorption Properties in Solvents of Different Polarities. Absorption maxima of the derivatives did not change much with changing solvents of different polarities (Figure 2 and 3). The spectra even remained almost unaltered for the molecule **1cd** which has a strong donor dimethyl amino group and strong acceptor nitrile moiety at the terminals of the butadiyne bridge, ruling out the possibility of its ground state dipole formation. The observations corroborate that all the fluorophores are presumably exposed to the same local environment in both ground and excited state, being completely noninteractive with the solvent environment within very short femtosecond absorption time scale. We were also highly elated to note the same UV-vis spectral trend among molecules in a particular solvent, discussed in an earlier section, not only for cyclohexane but also for all other solvents of different polarities. The parent molecule **1aa** absorbs at λ_{max} 323 nm in cyclohexane while the donor-acceptor based molecule **1cd** absorbs at λ_{max} 396 nm in cyclohexane. Thus simple tuning of electronic environment at the periphery of the butadiyne moiety allows opening a large absorption window. The absorption band spread over around 315 to 415 nm could be assigned to the $S_0 \rightarrow S_1$ transition whereas the region around 250 to 300 nm could be due to the $S_0 \rightarrow S_2$ transition. The derivatives **1ab**, **1bb**, and **1ad** have very high $S_0 \rightarrow S_2$ transition intensity along with the $S_0 \rightarrow S_1$ transition. On the other side, the $S_0 \rightarrow S_1$ transition for **1cc** and **1bc** intensifies at the cost of the absorption intensities of $S_0 \rightarrow S_2$ transition. Similar observation was found in some substituted amino containing butadiynyl derivatives reported by Shenoy et al.⁵⁸ The diyne **1cd** shows almost equal intensities of $S_0 \rightarrow S_1$ and $S_0 \rightarrow S_2$ transitions. Significant loss of vibrational fine structures has been registered for **1cd** on moving from non polar to

moderately polar to highly polar solvent, indicating the presence of strong ICT. The diyne **1cd** attracts special eyes when it is compared with its butadiene analogue, dimethylamino-cyano-diphenylbutadiene (DCB).⁵⁹ The derivative **1cd** absorbs at λ_{max} 385 nm in acetonitrile while DCB absorbs at 402 nm in acetonitrile. The data annotates the shorter molecular axis of **1cd** compared with the diene DCB.

Emission Properties in Solvents of Different Polarities. As our investigation proceeded, the emission spectral features in various solvents of different polarities had continued to puzzle us from molecule to molecule. The emission maxima for **1ab** and **1bb** do not change much with changing solvents of different polarities (Figure 4a, 4b). For example, the emission maxima for **1ab** are 441 nm in *n*-heptane and 457 nm in acetonitrile while 471 and 495 nm are those for **1bb** respectively. Thus, singly substituted methoxy to doubly substituted methoxy groups at the phenyl rings in **1ab** and **1bb** respectively procure a 30 nm red shift of emission maxima for *n*-heptane and 38 nm for acetonitrile. A close look at the emission spectra of **1ab** and **1bb** (Figure 4a, 4b) reveals a small structural emission part at around 400 nm. The emission maxima for **1ad** lie between 397 and 410 nm from *n*-heptane to acetonitrile exhibiting spectral insensitivity toward solvent polarities (Figure 4c). The emission profile for **1ad** is a little sharper at shorter wavelength but a long tail has been tailored to the longer wavelength. The emission maxima for **1ac** are considerably red-shifted as the solvent polarity rises. The effect of dimethyl amino group substituted phenyl ring as strong donor and unsubstituted phenyl ring as acceptor in **1ac** has been reflected in the shift of emission maxima from 446 nm in *n*-heptane to 526 nm in acetonitrile. The emission spectrum of **1ac** was observed to be very broad. The presence of two strong dimethyl amino groups in **1cc** furnished the emission spectrum as highly structured with a long tail emission at around 525 nm which is much more prominent for non polar *n*-heptane and cyclohexane. Thus moving from one dimethyl amino group

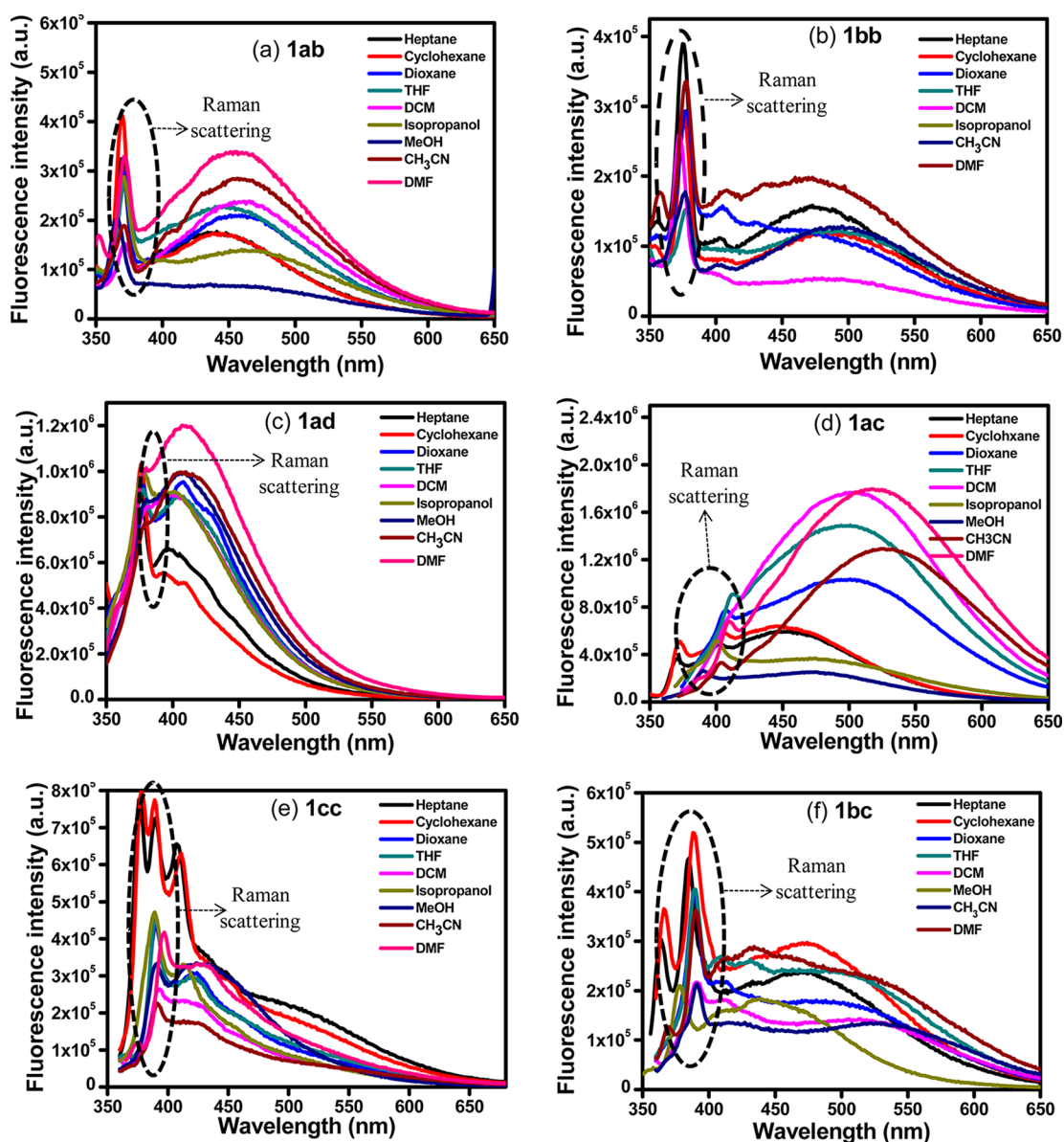


Figure 4. Emission spectra of (a) **1ab** ($\lambda_{\text{ex}} = 330$ nm), (b) **1bb** ($\lambda_{\text{ex}} = 340$ nm), (c) **1ad** ($\lambda_{\text{ex}} = 340$ nm), (d) **1ac** ($\lambda_{\text{ex}} = 330$ nm for cyclohexane and heptane, $\lambda_{\text{ex}} = 360$ nm for other solvents), (e) **1cc** ($\lambda_{\text{ex}} = 350$ nm), and (f) **1bc** ($\lambda_{\text{ex}} = 350$ nm) in different solvents (10^{-5} M). Dotted circle indicates Raman scattering.

bearing derivative **1ac** to two dimethyl amino groups substituted derivatives **1cc**, a drastic difference of emission spectral features was witnessed (Figure 4d, 4e). Widely separated dual emission was found for **1bc** where the locally excited (LE) state is at around 425 nm and the ICT state is at around 525 nm (Figure 4f). The fluorophore **1cd** attracted special attention owing to its unique emission spectral features compared to other fluorophores discussed here. The spectra of **1cd** were noticed to be structured in *n*-heptane and cyclohexane exhibiting emission maxima at 426 and 431 nm, respectively. The emission spectra exhibit a huge response in changing polarities of solvents (Figure 5a). The spectra are significantly red-shifted from non polar to polar solvents (Table 2). This implies that the excited state of **1cd** is comparatively more polar than its ground state and hence the excited state is more stabilized by polar solvents exhibiting a huge bathochromic shift. A very long emission tail extended to the higher wavelength for *n*-heptane and cyclohexane whereas a short

hump came up at shorter wavelength for solvents of moderate and high polarities in **1cd**. This observation shows dual fluorescence of **1cd** confirming emissions from both equilibrated LE and ICT states. The presence of an LE and a charge transfer state was suggested by Khundkar et al. in donor (MeS)-acceptor (CN) substituted butadiynyl derivative.¹¹ Guo and Xia et al. have also theoretically shown the involvement of a charge transfer state in donor-acceptor substituted α,ω -diphenylpolyynes.¹⁹ There is also a preminent finding for **1cd** in increase in Stokes' shift which is around 7419 cm^{-1} between *n*-heptane and acetonitrile. This large Stokes' shift is a consequence of efficient charge transfer from the donor dimethyl amino group to the acceptor nitrile moiety. It is also imperative to mention that quenching of fluorescence intensity took place in highly polar solvents. The photograph (Figure 5b) of **1cd** taken under UV light clearly shows the solvent induced Stoke's shift. The color ranges from blue in *n*-heptane ($\lambda_{\text{em}} = 426$ nm) to orange in DMF ($\lambda_{\text{em}} = 602$ nm).

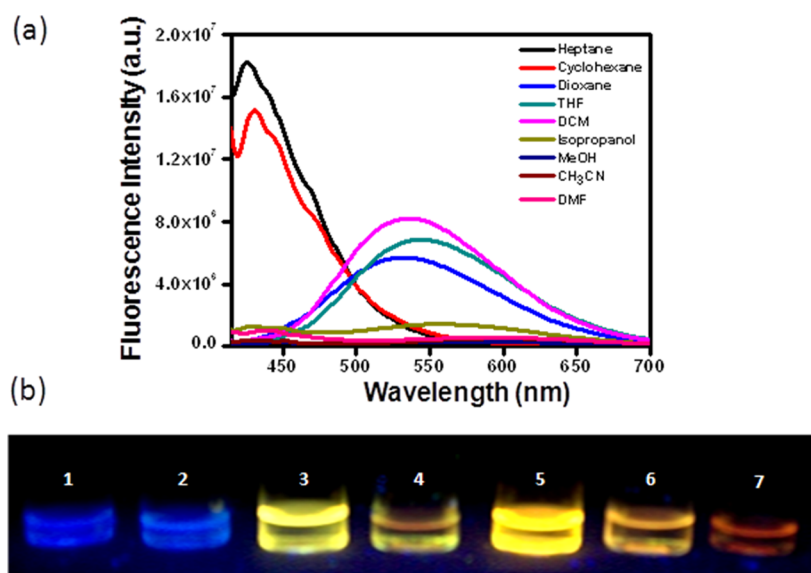


Figure 5. (a) Emission spectra of **1cd** in different solvents (1×10^{-5} M, $\lambda_{\text{ex}} = 390$ nm) and (b) photograph of **1cd** in different solvents under UV light, (1) *n*-heptane ($\lambda_{\text{em}} = 426$ nm); (2) cyclohexane ($\lambda_{\text{em}} = 431$ nm); (3) dioxane ($\lambda_{\text{em}} = 531$ nm); (4) methanol ($\lambda_{\text{em}} = 575$ nm); (5) THF ($\lambda_{\text{em}} = 545$ nm); (6) isopropanol ($\lambda_{\text{em}} = 559$ nm); (7) DMF ($\lambda_{\text{em}} = 602$ nm).

Table 2. Photophysical Parameters of 1cd in Different Solvents

solvents	λ_{abs} (longest absorption wavelength) nm	λ_{em} (max) (nm)	Stokes' shift (cm^{-1})	quantum yield
(1) heptane	393	426	1971	0.03
(2) cyclohexane	396	431	2051	0.03
(3) dioxane	389	531	6874	0.11
(4) THF	389	545	7358	0.11
(5) DCM	390	537	7019	0.11
(6) isopropanol	385	559	8085	0.02
(7) MeOH	383	575	8718	0.02
(8) CH_3CN	385	603	9390	0.02
(9) DMF	393	602	8834	0.02

The quantum yield of the molecule **1cd** was recorded with respect to quinine sulfate. The data in Table 2 shows that the value decreases with an increase in solvent polarity. The lower quantum yield in the highly polar solvent could be due to the formation of the ICT state which would result in nonradiative decay in the excited state. The change in dipole moment between the excited and ground states of **1cd** was obtained from the slope of Lippert–Mataga plot^{60,61} which was found to be about 35.2 D assuming Onsager radius as 8.14 Å. The Onsager radius was calculated as half of the distance between nitrogen of donor dimethyl amino group and nitrogen of acceptor nitrile moiety in the optimized geometry of the molecule **1cd** using B3LYP/6-31G* DFT^{62,63} geometry optimization calculation using the Gaussian 03 computational package.⁶⁴ This result assures the high polar nature of the fluorophore **1cd** due to ICT aided by the two alkynyl bridges between the donor dimethyl amino and acceptor nitrile moieties.

Origin of Asymmetry of Emission Spectra. The asymmetry of emission spectral features among various fluorophores under study triggered us to understand its origin. We anticipated that the emission spectra of all the fluorophores

are composed of both an LE and an ICT state. Thus simultaneous appearance of an LE and ICT state is solely the characteristic outcome of conjugated diyne, regardless of the electronic environment at the periphery of the diyne moiety. The electronic environment may only affect the position and intensity of the two states depending on the chemical environment, thereby mystifying the emission features from molecule to molecule. To simplify our thoughts, all the emission spectra were fitted into multiple Gaussians. Generally, standard emission spectral profiles have Gaussian shape^{30,65} while spectral profiles of Raman scattering as well as vibrational lines resemble the Lorentzian shape.^{66–68} As many of the emission spectra are structured because of vibronic spectral lines of LEs, and in many cases Raman scattering is very close to fluorescence maxima, Gaussian fitting was found to be troublesome in some of the molecules. In these cases, the problem could be circumvented by using multiple Lorentzians fitting of the emission spectrum. Major parts of Gaussian and Lorentzian bands are the same, and the Lorentzian curve differs from the Gaussian curve in the fact that the Lorentzian curve has a long tail compared to the Gaussian one as stated by Meier.⁶⁹ It is pertinent to mention that this difference really does not hamper our study of interest. As expected, multiple Gaussian/Lorentzian fitting has unravelled the emission spectra by resolving it as a mixture of multiple emission bands. The shorter wavelength bands could be assigned to a LE which was again split into vibronic spectra whereas the longer wavelength band or tail could be due to ICT. The derivatives **1ab** and **1ad** have been chosen here as representatives to show the Gaussian/Lorentzian fitted curves (Figure 6, 7). The presence of Raman line was observed in all the fluorescence spectra recorded, which was identified by the usual procedure of recording the fluorescence spectrum at different excitation wavelength. Since the locally excited emission band showed vibronic structuring, it was necessary to carefully identify and remove the Raman band for the further analysis of the spectral profiles. Figure 8 shows that the resolved longer wavelength ICT band for **1ab** and **1ad** is red-shifted with changing solvents of increasing polarities. As for illustration, emission maxima of

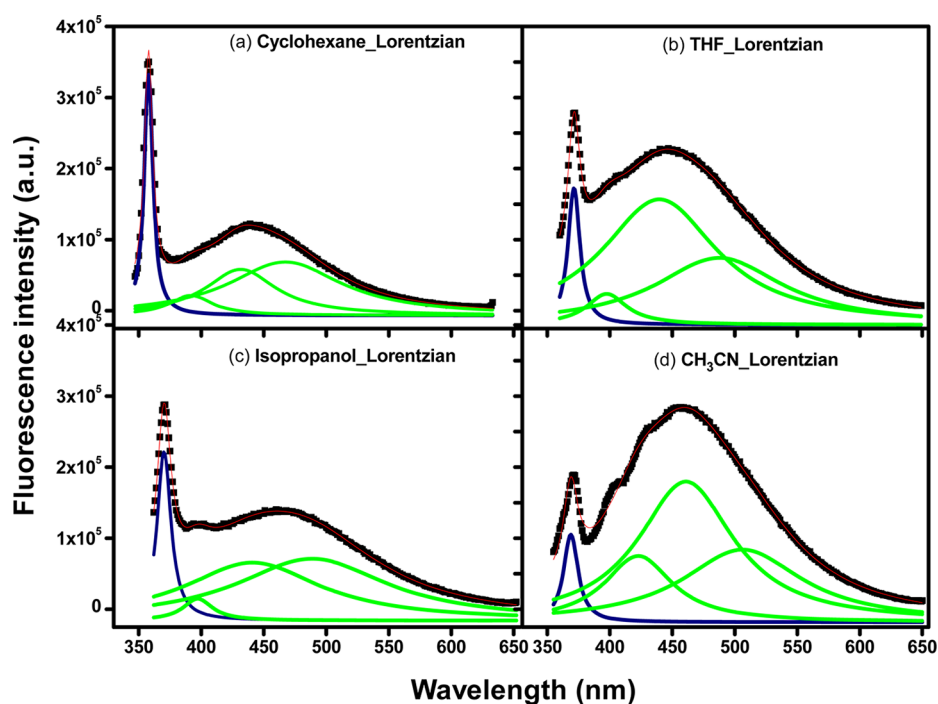


Figure 6. Lorentzian fitting of emission spectra of **1ab** (blue peak indicates Raman scattering).

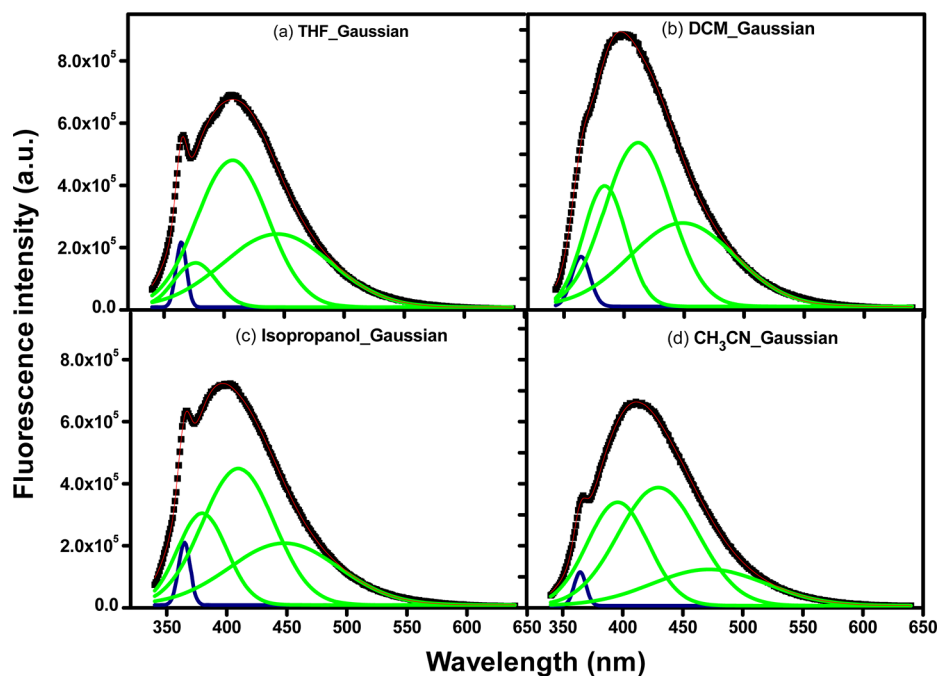


Figure 7. Gaussian fitting of emission spectra of **1ad** (blue peak indicates Raman scattering).

fitted ICT band for **1ab** have been found to be 462 nm in *n*-heptane and 506 nm in acetonitrile whereas those are 427 nm in *n*-heptane and 472 nm in acetonitrile for **1ad**. The shorter wavelength bands for **1ab** and **1ad** have been resolved into a mixture of vibronic spectrum. Pleasingly, the energy gap obtained from the difference of the maxima of two vibronic spectra has been found to be around 2000 cm^{-1} which is unambiguously assigned to C–C triple bond stretching of butadiynyl moiety,²⁷ comparing its value with the experimental and theoretical values (Table 3). The LEs, wherever possible for the derivatives, have been resolved into vibronic spectra (see

Supporting Information), and the calculated infrared stretching frequency has been found to be almost consistent with the former value. Thus, the observed association of C–C triple bond stretching frequency with the electronic transition corresponding to the LE state is important as it provides a spectroscopic evidence for the participation of the butadiyne moiety in electronic transition.

Our effort was further directed at finding the quantum yields of **1ab** and **1ad** from the area of the Gaussian/Lorentzian fitted emission profiles (Figure 6 and 7). The calculated quantum yields of **1cd** have been considered as standard to find out the

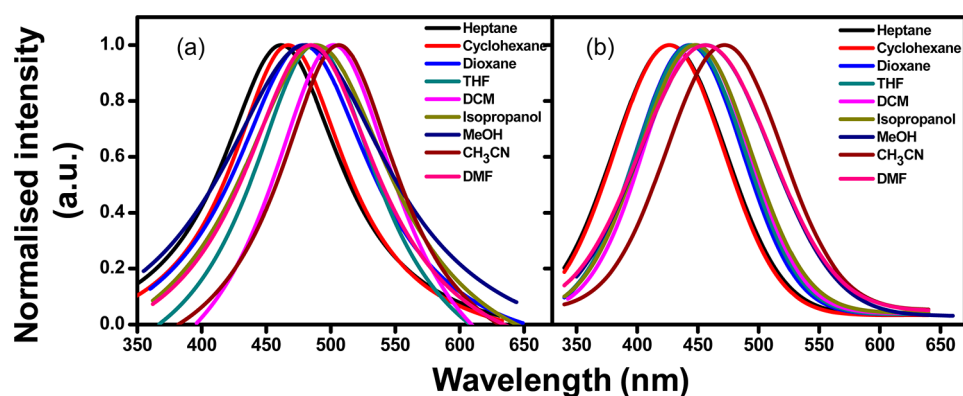


Figure 8. Normalized longer wavelength emission spectra (from the fitted curves) of (a) **1ab** and (b) **1ad**.

Table 3. IR Stretching Frequency for C–C Triple Bond

derivatives	IR values for C–C triple bond		
	theoretical value ^a (cm ⁻¹)	experimental value ^b (cm ⁻¹)	value obtained from vibronic progression ^c (cm ⁻¹)
1ab	2318	2206	
	2245	2145	2273
1ad	2317	2210	
	2245	2137	2023

^aB3LYP/6-31g*. ^bFT-IR. ^cIn cyclohexane.

quantum yields of **1ab** and **1ad**. The data has been tabulated in Table 4 which shows very low quantum yield for the derivatives. Table 4 shows that ICT has significant contribution to the total quantum yield for both derivatives **1ab** and **1ad**. The contribution of ICT to the overall quantum yield in derivative **1ab**, having one methoxy group as donor, is much higher than that of the LE contribution. Fluorophores containing bulkier aromatic groups at the periphery of the diyne have been found to have higher or reasonably higher quantum yield in the literature.^{13–16,22,35} Thus our data prompted us to conclude that the diyne moiety really does not play an integral role in enhancing quantum yield; rather it is the peripheral moieties which control the quantum yield. Here phenyl rings being situated at the periphery of the diyne hardly help to increase the quantum yield value of the derivatives.

The λ_{max} values obtained from the resolved ICT bands were used to understand the solvation dynamics of the fluorophores **1ab** and **1ad**. The values were fitted well in $E_{\text{T}}(30)^{70}$ plot where polar protic solvents like isopropanol and methanol

follow a different trend than aprotic solvents (Figure 9). Similar trends have been observed and attributed to the changes in the character of emissive states.^{71,72} Attempts to fit the data in a Kamlet Taft^{73–75} plot were not successful.

Fluorescence Lifetime Studies. To attest the concurrent existence of an LE and an ICT state, a time-resolved fluorescence dynamic study was carried out. The fluorophore **1cd** was taken here as a molecule of choice to accomplish this study. The experiment was performed in various solvents of different polarities, and fluorescence lifetime was collected at different emissions which have been shown in Figure 10. Non polar solvents like *n*-heptane and cyclohexane fit well in monoexponential decay when lifetime is collected at λ_{em} 426 nm whereas they show biexponential behavior when lifetime is collected at λ_{em} 492 and 537 nm. The amplitude of the two states also changes accordingly while going from 426 to 492 to 537 nm (Table 5). Moderately polar solvent tetrahydrofuran (THF) and dichloromethane (DCM) exhibit biexponential behavior at λ_{em} 426 nm while they start showing monoexponential behavior from λ_{em} 492 to 537 to 605 nm. The amplitude in THF and DCM at different emissions also changes accordingly. On the other hand, in isopropanol and acetonitrile the lifetimes are found to be biexponential at all the emission points. These results confirm the excited state equilibrium between an LE and an ICT state. The lifetime is less than 1 ns in *n*-heptane and cyclohexane while in THF and DCM it is little more than 1 ns. The lifetime is even lower in highly polar solvents such as isopropanol and acetonitrile. The low lifetime data undoubtedly indicates the association of an ICT state in the excited state.

Table 4. Quantum Yield for **1ab** and **1ad** Calculated from the Area of Fitted Emission Spectra (The data in the parenthesis indicates the contribution of Φ_{Local} or Φ_{ICT} to the Φ_{Total})

solvents	quantum yield ($\Phi \times 10^{-3}$)					
	1ab			1ad		
	$\Phi_{\text{Local}} \times 10^{-3}$	$\Phi_{\text{ICT}} \times 10^{-3}$	$\Phi_{\text{Total}} \times 10^{-3}$	$\Phi_{\text{Local}} \times 10^{-3}$	$\Phi_{\text{ICT}} \times 10^{-3}$	$\Phi_{\text{Total}} \times 10^{-3}$
(1) heptane	1.8 (0.27)	4.8 (0.73)	6.6	4.7 (0.52)	4.4 (0.48)	9.1
(2) cyclohexane	2.4 (0.39)	3.8 (0.61)	6.2	3.4 (0.52)	3.1 (0.48)	6.5
(3) dioxane	1.0 (0.26)	2.8 (0.74)	3.8	6.6 (0.63)	3.9 (0.37)	10.5
(4) THF	1.6 (0.31)	3.5 (0.69)	5.1	7.0 (0.64)	3.7 (0.35)	10.7
(5) DCM	1.4 (0.30)	3.3 (0.70)	4.7	8.1 (0.70)	3.5 (0.30)	11.6
(6) isopropanol	1.4 (0.20)	5.5 (0.80)	6.9	6.3 (0.68)	3.0 (0.32)	9.3
(7) MeOH	1.1 (0.19)	4.7 (0.81)	5.8	5.1 (0.58)	3.7 (0.42)	8.8
(8) CH ₃ CN	1.4 (0.20)	5.6 (0.80)	7.0	9.5 (0.73)	3.6 (0.27)	13.1
(9) DMF	1.5 (0.24)	4.8 (0.76)	6.3	9.4 (0.69)	4.2 (0.31)	13.6

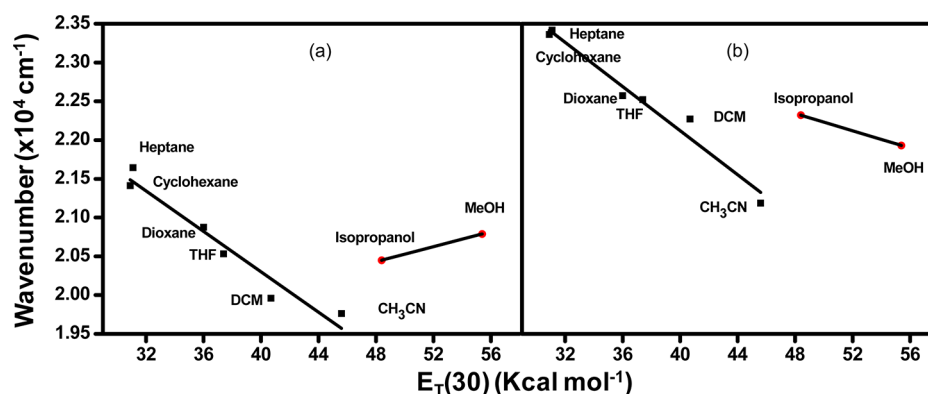


Figure 9. $E_T(30)$ plots for (a) **1ab**, and (b) **1ad** using resolved ICT data.

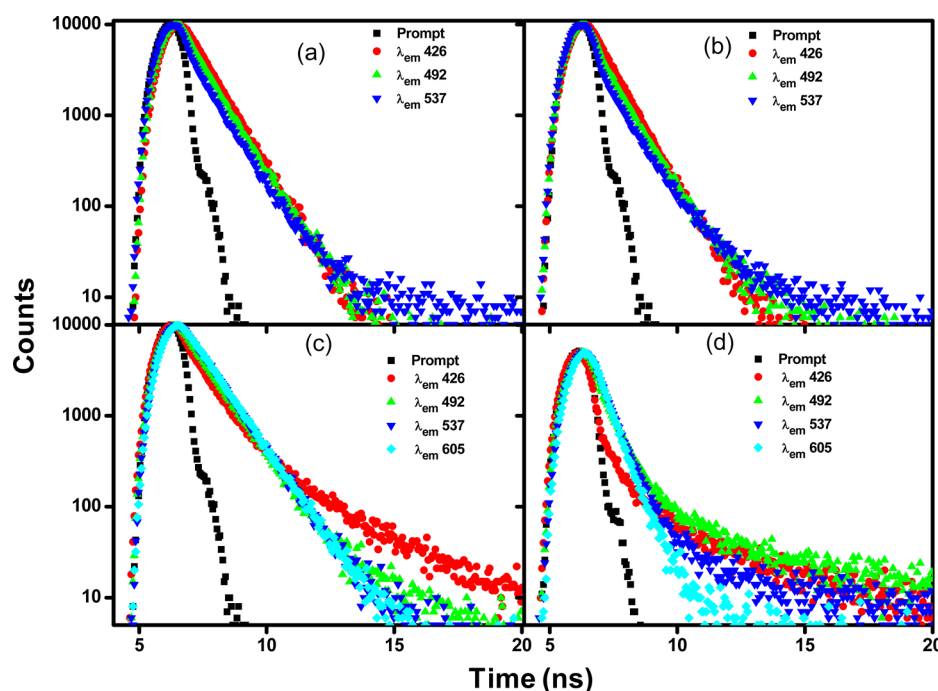


Figure 10. Lifetime profile of **1cd** at different emissions in (a) heptane, (b) cyclohexane, (c) THF, and (d) acetonitrile.

Theoretical Investigations. To gain further insights into the electronic transition of the fluorophores theoretical calculations using density functional theory with the B3LYP hybrid functional and 6-31g* basis set were performed.^{62,63} Figure 11 represents the molecular orbitals involving the first singlet vertical transition of **1cd** as the representative. The $S_0 \rightarrow S_1$ transition mainly involves transitions from the highest occupied molecular orbital (HOMO) to the lowest unoccupied molecular orbital (LUMO) for all the derivatives. It is noted that the HOMO of the molecule **1cd** is substantially localized on the dimethyl amino group substituted phenyl ring and butadiyne moiety with lesser electronic distribution on the nitrile containing phenyl ring. On the other hand, the LUMO of **1cd** is highly concentrated on the phenyl ring having a nitrile group and butadiyne bridge with small extension of electron density to the dimethyl amino substituted phenyl ring. A similar nature of the HOMO and LUMO is observed for neutral-donor **1ab**, neutral-acceptor **1ad**, and neutral-donor **1ac** derivatives. For the donor–donor derivatives **1bb**, **1bc**, and **1cc**, the HOMO is centered on both the donor substituted phenyl rings along with butadiyne bridge whereas the LUMO is distributed

over the butadiyne moiety with less electronic distribution on donor substituted phenyl rings. Thus a HOMO to LUMO transition corresponds to the charge transfer state. Albeit the HOMO to LUMO transition mainly contributes to the $S_0 \rightarrow S_1$ transition, the minor contribution can not be ignored given the fact that it involves molecular orbitals with electron density solely localized on the diyne moiety. This observation is unique for all the butadiynyl derivatives (see Supporting Information). Thus all electronic transitions are controlled by the same orbitals and as a consequence, structured absorption and local emission are observed for the butadiynyl derivatives.

The mixing up of orbitals contributing to an ICT and LE state clearly explains our experimental observation of emissions from both the LE and the ICT state for all the fluorophores. Figure 12 shows that orbital contribution to the ICT state is much higher than the LE state. Moving from neutral **1aa** to the donor–acceptor **1cd** derivative, the orbital contribution to the ICT state increases. On the other hand, moving from donor–acceptor **1cd** to neutral **1aa** derivative, the orbital contribution to the LE state starts rising. At this point, it is worth stressing that the observed trend of the orbital contribution to the ICT

Table 5. TCSPC Experimental Data of 1cd in Different Solvents at Different Emissions

solvents	lifetime collected at different emission wavelengths using 370 nm LED								
	426 nm		492 nm		537 nm		605 nm		
	τ_1 (ns) (B1)	τ_2 (ns) (B2)	CHISQ	τ_1 (ns) (B1)	τ_2 (ns) (B2)	CHISQ	τ_1 (ns) (B1)	τ_2 (ns) (B2)	CHISQ
heptane	0.90 (1)		1.24	0.23 (0.17)	0.94 (0.83)	1.00	0.14 (0.44)	0.90 (0.56)	1.17
cyclohexane	0.85 (1)		1.21	0.16 (0.43)	0.94 (0.57)	1.23	0.12 (0.64)	0.99 (0.36)	1.13
THF	0.74 (0.71)	1.86 (0.29)	1.27	1.04 (1)		1.04	1.06		1.26
DCM	0.15 (0.60)	1.31 (0.40)	1.12	1.22 (1)		1.14	1.25 (1)		1.22
isopropanol	0.04 (0.95)	1.15 (0.05)	1.29	0.15 (0.68)	0.63 (0.32)	1.23	0.31 (0.73)	0.69 (0.27)	1.27
CH ₃ CN	0.06 (0.88)	1.16 (0.12)	1.17	0.14 (0.48)	0.73 (0.52)	1.03	0.46 (0.89)	1.50 (0.11)	1.02

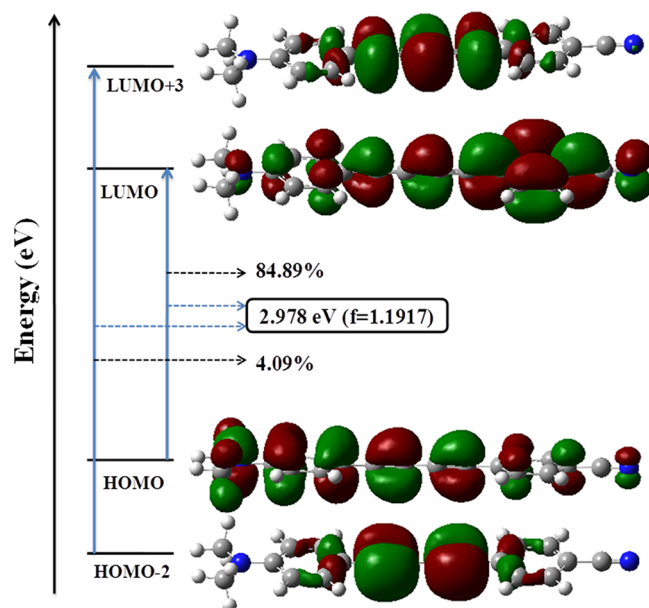


Figure 11. Frontier orbitals of 1cd for the first singlet vertical transition.

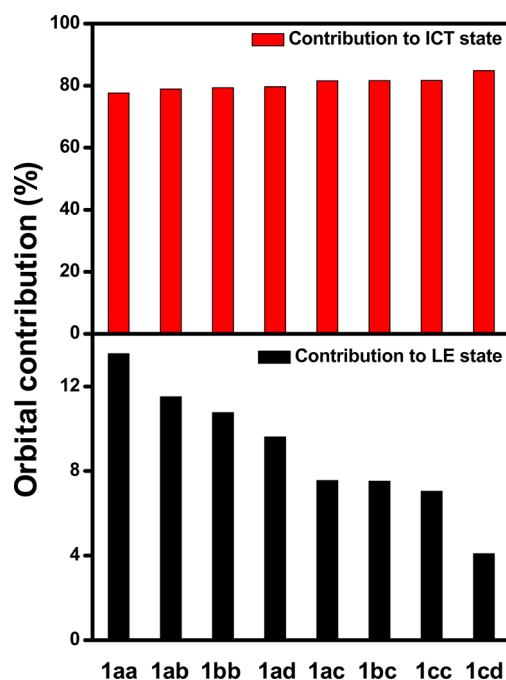


Figure 12. Orbital contribution for LE and ICT state of 1aa–1cd.

state from molecule to molecule (Figure 12) is almost in similar agreement with our experimental finding of a gradual red shift of the onset of the electronic absorption spectra (Figure 1a) from neutral to donor–donor to donor–acceptor molecules. The electronic distribution in LUMO+3 and HOMO-2 in 1cd is noteworthy. Here, in 1cd, the electronic distribution is parallel to the phenyl rings whereas it is perpendicular to the phenyl rings for HOMO and LUMO orbitals.⁷⁶ Orita and Otera et al. found similar observation for the NH₂-yne-tri-yne derivative.¹⁵

CONCLUSIONS

In summary, quick access to a series of diphenyl butadiynyl derivatives has been achieved through microwave assisted Eglinton coupling of terminal alkynes. A systematic and detailed study solely focused on the evaluation of fundamental photophysics of the “butadiyne” core moiety has been accomplished. Several important findings emerged through the evaluation of photophysical properties of these butadiynyl fluorophores.

(1) The fluorophores exhibit emission from both an LE and an ICT state. Especially, ICT in donor–donor systems is really a remarkable observation.

(2) The pure ICT emission has been successfully separated from pure LE emission using Gaussian/Lorentzian curve fitting.

(3) The vibronic progression of the LE transition corresponds to the C–C stretching of the diyne moiety, clearly providing spectroscopic evidence that there is a strong contribution of this moiety to the LE transition. This conclusion is substantiated by theoretical calculation.

(4) Judicious tuning of electronics at the phenyl rings has opened a very long emission window for this class of fluorophores. Moreover, the fluorophore containing a donor dimethyl amino group and acceptor nitrile moiety attracts extra attention considering the fact that the fluorophore resembles the extended version of the literature celebrity twisted ICT probe dimethyl amino benzonitrile (DMBN).

(5) The derivatives appear to conform to other established photophysical behaviors like solvatochromism, Stokes' shift, and fluorescence intensity.

The presence of two acetylenic moieties in all the fluorophores gains an extra advantage over double bonds because of the absence of cis-trans isomerization. Low quantum yields of the derivatives are not a matter of concern for the present study since it could easily be increased by just tuning the periphery of the diyne, and such studies are underway in our laboratory. Thus we believe that our study has opened new avenues for the generation of new advanced fluorophores based on the fundamental photophysics of the diyne core, and it has provided a recipe to analyze the fundamental photophysics of this same class of all existing fluorophores in the literature.

ASSOCIATED CONTENT

Supporting Information

General experimental methods, synthetic procedures and characterization data for all the butadiynyl derivatives, Lorentzian fitting of emission spectra, frontier orbitals for the first singlet vertical transition of fluorophores. This material is available free of charge via the Internet at <http://pubs.acs.org>.

AUTHOR INFORMATION

Corresponding Author

*E-mail: sjgharpure@iitb.ac.in (S.J.G.), mishra@iitm.ac.in (A.K.M.). Phone: +91-22-2576 7171 (S.J.G.), +91-44-22574207 (A.K.M.). Fax: +91-22-2576 7152 (S.J.G.), +91-44-22574202 (A.K.M.).

Notes

The authors declare no competing financial interest.

ACKNOWLEDGMENTS

The authors thank CSIR, DBT, and DST, New Delhi, for financial support. The high performance computing facility of IIT Madras is greatly acknowledged. A.K.P. and M.M. thank

CSIR, New Delhi, for research fellowships. A.K.P. thanks Mr. V. Prasath, IIT Bombay, for helpful discussion.

REFERENCES

- (1) Meijer, E. J.; Tanase, C.; Blom, P. W. M.; van Veenendaal, E.; Huisman, B.-H.; de Leeuw, D. M.; Klapwijk, T. M. Switch-On Voltage in Disordered Organic Field-Effect Transistors. *Appl. Phys. Lett.* **2002**, *80*, 3838–3840.
- (2) Brown, A. R.; Pomp, A.; Hart, C. M.; de Leeuw, D. M. Logic Gates Made from Polymer Transistors and Their Use in Ring Oscillators. *Science* **1995**, *270*, 972–974.
- (3) Goes, M.; Verhoeven, J. W.; Hofstraat, H.; Brunner, K. OLED and PLED Devices Employing Electrogenerated, Intramolecular Charge-Transfer Fluorescence. *ChemPhysChem* **2003**, *4*, 349–358.
- (4) Kraft, A.; Grimsdale, A. C.; Holmes, A. B. Electroluminescent Conjugated Polymers—Seeing Polymers in a New Light. *Angew. Chem., Int. Ed.* **1998**, *37*, 403–428.
- (5) Badugu, R.; Lakowicz, J. R.; Geddes, C. D. Enhanced Fluorescence Cyanide Detection at Physiologically Lethal Levels: Reduced ICT-Based Signal Transduction. *J. Am. Chem. Soc.* **2005**, *127*, 3635–3641.
- (6) Yukruk, F.; Akkaya, E. U. Modulation of Internal Charge Transfer (ICT) in a Bay Region Hydroxylated Peryleneimide (PDI) Chromophore: A Chromogenic Chemosensor for pH. *Tetrahedron Lett.* **2005**, *46*, 5931–5933.
- (7) Swinburne, A. N.; Paterson, M. J.; Beeby, A.; Steed, J. W. Fluorescent Twist-On Sensing by Induced-Fit Anion Stabilisation of a Planar Chromophore. *Chem.—Eur. J.* **2010**, *16*, 2714–2718.
- (8) Cowley, D. J. Protein structure: Polar Pocket with Nonpolar Lining. *Nature* **1986**, *319*, 14–15.
- (9) Rettig, W. Charge Separation in Excited States of Decoupled Systems—TICT Compounds and Implications Regarding the Development of New Laser Dyes and the Primary Process of Vision and Photosynthesis. *Angew. Chem., Int. Ed. Engl.* **1986**, *25*, 971–988.
- (10) Bonačić-Koutecký, V.; Koutecký, J.; Michl, J. Neutral and Charged Biradicals, Zwitterions, Funnel in S₁, and Proton Translocation: Their Role in Photochemistry, Photophysics, and Vision. *Angew. Chem., Int. Ed. Engl.* **1987**, *26*, 170–189.
- (11) Biswas, M.; Nguyen, P.; Marder, T. B.; Khundkar, L. R. Unusual Size Dependence of Nonradiative Charge Recombination Rates in Acetylene-Bridged Compounds. *J. Phys. Chem. A* **1997**, *101*, 1689–1695.
- (12) Stiegman, A. E.; Graham, E.; Perry, K. J.; Khundkar, L. R.; Cheng, L.-T.; Perry, J. W. The Electronic Structure and Second-Order Nonlinear Optical Properties of Donor-Acceptor Acetylenes: A Detailed Investigation of Structure-Property Relationships. *J. Am. Chem. Soc.* **1991**, *113*, 7658–7666.
- (13) Wang, C.; Pålsson, L.-O.; Batsanov, A. S.; Bryce, M. R. Molecular Wires Comprising π -Extended Ethynyl- and Butadiynyl-2,5-Diphenyl-1,3,4-Oxadiazole Derivatives: Synthesis, Redox, Structural, and Optoelectronic Properties. *J. Am. Chem. Soc.* **2006**, *128*, 3789–3799.
- (14) Pålsson, L.-O.; Wang, C.; Batsanov, A. S.; King, S. M.; Beeby, A.; Monkman, A. P.; Bryce, M. R. Efficient Intramolecular Charge Transfer in Oligoene-Linked Donor- π -Acceptor Molecules. *Chem.—Eur. J.* **2010**, *16*, 1470–1479.
- (15) Fang, J.-K.; An, D.-L.; Wakamatsu, K.; Ishikawa, T.; Iwanaga, T.; Toyota, S.; Matsuo, D.; Orita, A.; Otera, J. Synthesis and Spectroscopic Study of Diphenylamino-Substituted Phenylene-(poly)ethynylenes: Remarkable Effect of Acetylenic Conjugation Modes. *Tetrahedron Lett.* **2010**, *51*, 917–920.
- (16) Fang, J.-K.; An, D.-L.; Wakamatsu, K.; Ishikawa, T.; Iwanaga, T.; Toyota, S.; Akita, S.-I.; Matsuo, D.; Orita, A.; Otera, J. Synthesis and Spectroscopic Study of Phenylene-(poly)ethynylenes Substituted by Amino or Amino/Cyano Groups at Terminal(s): Electronic Effect of Cyano Group on Charge-Transfer Excitation of Acetylenic π -systems. *Tetrahedron* **2010**, *66*, 5479–5485.

- (17) Akiyama, S.; Nakasuji, K.; Akashi, K.; Nakagawa, M. On the Electronic Spectra of Some α,ω -Diarylpolyynes. *Tetrahedron Lett.* **1968**, *9*, 1121–1126.
- (18) Nakagawa, M.; Akiyama, S.; Nakasuji, K.; Nishimoto, K. Novel Linear Relation in the Electronic Spectra of α,ω -Diarylpolyynes. *Tetrahedron* **1971**, *27*, 5401–5418.
- (19) Ma, X.; Yan, L.; Wang, X.; Guo, Q.; Xia, A. Spectral and Intramolecular Charge Transfer Properties in Terminal Donor/Acceptor-Substituted All-trans- α,ω -Diphenylpolyenes and α,ω -Diphenylpolyynes. *Phys. Chem. Chem. Phys.* **2011**, *13*, 17273–17283.
- (20) Marsden, J. A.; Miller, J. J.; Shirtcliff, L. D.; Haley, M. M. Structure–Property Relationships of Donor/Acceptor-Functionalized Tetrakis(phenylethynyl)benzenes and Bis(dehydrobenzoannuleno)benzenes. *J. Am. Chem. Soc.* **2005**, *127*, 2464–2476.
- (21) Spitler, E. L.; Haley, M. M. Synthesis and Structure–Property Relationships of Donor/Acceptor-Functionalized bis-(dehydrobenzo[18]annuleno)benzenes. *Org. Biomol. Chem.* **2008**, *6*, 1569–1576.
- (22) Benniston, A. C.; Harriman, A.; Lawrie, D. J.; Rostron, S. A. A Closely-Coupled Pyrene Dimer Having Unusually Intense Fluorescence. *Eur. J. Org. Chem.* **2004**, 2272–2276.
- (23) Kwon, J. H.; Lee, S. T.; Shim, S. C. Photochemistry of 1-Aryl-4-(pentamethylsilyl)-1,3-butadiynes. *J. Org. Chem.* **1994**, *59*, 1108–1114.
- (24) Armitage, J. B.; Entwistle, N.; Jones, E. R. H.; Whiting, M. C. Researches on Acetylenic Compounds. XLI. The synthesis of Diphenylpolyacetylenes. *J. Chem. Soc.* **1954**, 147–154.
- (25) Beer, M. Electronic Spectra of Polyacetylenes. *J. Chem. Phys.* **1956**, *25*, 745–750.
- (26) Hirata, Y.; Okada, T.; Nomoto, T. Photophysical Properties of Diphenylacetylene Derivatives in the Solution Phase: Comparison with the Dynamical Properties of Diphenylbutadiyne. *Chem. Phys. Lett.* **1998**, *293*, 371–377.
- (27) Nagano, Y.; Ikoma, T.; Akiyama, K.; Tero-Kubota, S. Symmetry Switching of the Fluorescent Excited State in α,ω -Diphenylpolyynes. *J. Am. Chem. Soc.* **2003**, *125*, 14103–14112.
- (28) Sekher, P.; Talwar, S. S.; Kamath, M. B.; Babu, K. N. Emission Studies of 1,4-bis(heteroaryl)-1,3-butadiynes. *J. Photochem. Photobiol. A* **1990**, *55*, 71–86.
- (29) Xing, Y.; Xu, X.; Zhang, P.; Tian, W.; Yu, G.; Lu, P.; Liu, Y.; Zhu, D. Carbazole-Pyrene-Based Organic Emitters for Electroluminescent Device. *Chem. Phys. Lett.* **2005**, *408*, 169–173.
- (30) Cataldo, F.; Ravagnan, L.; Cinquanta, E.; Castelli, I. E.; Manini, N.; Onida, G.; Milani, P. Synthesis, Characterization, and Modeling of Naphthyl-Terminated sp Carbon Chains: Dinaphthylpolyynes. *J. Phys. Chem. B* **2010**, *114*, 14834–14841.
- (31) Egbe, D. A. M.; Birkner, E.; Klemm, E. Highly Luminescent Diyne Containing Hybrid Polyphenyleneethynylene/Poly(p-phenylenevinylene) Polymer: Synthesis and Characterization. *J. Polym. Sci. Part A: Polym. Chem.* **2002**, *40*, 2670–2679.
- (32) Rodriguez, J. G.; Tejedor, J. L.; Rumbero, A.; Canoira, L. Stereospecific Synthesis of Conjugated (1E,3E)- and (1Z,3Z)-1,4-di(n-N,N-dimethylaminophenyl)-1,3-butadienes from 2-chloro-1-(n-N,N-dimethylaminophenyl)ethenes: Fluorescence Properties. *Tetrahedron* **2006**, *62*, 3075–3080.
- (33) Adhikari, R. M.; Duan, L.; Hou, L.; Qiu, Y.; Neckers, D. C.; Shah, B. K. Ethynylphenyl-Linked Carbazoles as a Single-Emitting Component for White Organic Light-Emitting Diodes. *Chem. Mater.* **2009**, *21*, 4638–4644.
- (34) Kang, Y.; Wang, S. Syntheses and Photophysical Properties of Rigid-Rod Conjugated Compounds Based on N-7-Azaindole and 2,2'-Dipyridylamine. *Tetrahedron Lett.* **2002**, *43*, 3711–3713.
- (35) Kato, S.-I.; Noguchi, H.; Kobayashi, A.; Yoshihara, T.; Tobita, S.; Nakamura, Y. Bicarbazoles: Systematic Structure–Property Investigations on a Series of Conjugated Carbazole Dimers. *J. Org. Chem.* **2012**, *77*, 9120–9133.
- (36) Michl, J.; Sykes, E. C. H. Molecular Rotors and Motors: Recent Advances and Future Challenges. *ACS Nano* **2009**, *3*, 1042–1048.
- (37) Kottas, G. S.; Clarke, L. I.; Horinek, D.; Michl, J. Artificial Molecular Rotors. *Chem. Rev.* **2005**, *105*, 1281–1376.
- (38) Wu, S.-T.; Meng, H.-H. B.; Dalton, L. R. Diphenyl-Diacetylene Liquid Crystals for Electro-Optic Application. *J. Appl. Phys.* **1991**, *70*, 3013–3017.
- (39) Wu, S.-T.; Margerum, J. D.; Meng, H. B.; Dalton, L. R.; Hsu, C.-S.; Lung, S.-H. Room-Temperature Diphenyl-Diacetylene Liquid Crystals. *Appl. Phys. Lett.* **1992**, *61*, 630–632.
- (40) Wu, S.-T.; Neubert, M. E.; Keast, S. S.; Abdallah, D. G.; Lee, S. N.; Walsh, M. E.; Dorschner, T. A. Wide Nematic Range Alkenyl Diphenyldiacetylene Liquid Crystals. *Appl. Phys. Lett.* **2000**, *77*, 957–959.
- (41) Beristain, M. F.; Ogawa, T.; Gomez-Sosa, G.; Munoz, E.; Maekawa, Y.; Halim, F.; Smith, F.; Walsler, A.; Dorsinville, R. Polymerization of Diphenylbutadiyne by Gamma Rays Irradiation in the Molten State. *Mol. Cryst. Liq. Cryst.* **2010**, *521*, 237–245.
- (42) Sari, O.; Roy, V.; Balzarini, J.; Snoeck, R.; Andrei, G.; Agrofoglio, L. A. Synthesis and Antiviral Evaluation of C5-Substituted-(1,3-diyne)-2'-deoxyuridines. *Eur. J. Med. Chem.* **2012**, *53*, 220–228.
- (43) Shun, A. L. K. S.; Tykwinski, R. R. Synthesis of Naturally Occurring Polyynes. *Angew. Chem., Int. Ed.* **2006**, *45*, 1034–1057.
- (44) Glaser, C. Beiträge zur Kenntniss des Acetenylbenzols. *Ber. Dtsch. Chem. Ges.* **1869**, *2*, 422–424.
- (45) Eglinton, G.; Galbraith, A. R. Macrocyclic Acetylenic Compounds. I. Cyclotetradeca-1,3-diyne and Related Compounds. *J. Chem. Soc.* **1959**, 889–896.
- (46) Hay, A. S. Oxidative Coupling of Acetylenes. *J. Org. Chem.* **1960**, *25*, 1275–1276.
- (47) Hay, A. S. Oxidative Coupling of Acetylenes. II. *J. Org. Chem.* **1962**, *27*, 3320–3321.
- (48) Chodkiewicz, W. Synthesis of Acetylenic Compounds. *Ann. Chim. Paris* **1957**, *2*, 819–869.
- (49) Cadiot, P.; Chodkiewicz, W. In *Chemistry of Acetylenes*; Viehe, H. G., Ed.; Marcel Dekker: New York, 1969; pp 597–647.
- (50) Sonogashira, K.; Tohda, Y.; Hagihara, N. Convenient Synthesis of Acetylenes. Catalytic Substitutions of Acetylenic Hydrogen with Bromo Alkenes, Iodo Arenes, and Bromopyridines. *Tetrahedron Lett.* **1975**, 4467–4470.
- (51) Takahashi, S.; Kuroyama, Y.; Sonogashira, K.; Hagihara, N. A Convenient Synthesis of Ethynylarenes and Diethynylarenes. *Synthesis* **1980**, 627–630.
- (52) For a review on acetylenic couplings see: Siemsen, P.; Livingston, R. C.; Diederich, F. Acetylenic Coupling: A Powerful Tool in Molecular Construction. *Angew. Chem., Int. Ed.* **2000**, *39*, 2632–2657.
- (53) Sharifi, A.; Mirzaei, M.; Naimi-Jamal, M. R. Copper-Catalyzed Oxidative Homo-Coupling of Terminal Acetylenes on Alumina Assisted by Microwave Irradiation. *J. Chem. Res.* **2002**, 628–630.
- (54) Corey, E. J.; Fuchs, P. L. A Synthetic Method for Formyl→Ethynyl Conversion (RCHO→RCCH or RCCR'). *Tetrahedron Lett.* **1972**, *13*, 3769–3772.
- (55) Michel, P.; Gennet, D.; Rassat, A. A One-Pot Procedure for the Synthesis of Alkynes and Bromoalkynes from Aldehydes. *Tetrahedron Lett.* **1999**, *40*, 8575–8578.
- (56) Beshai, M.; Dhudshia, B.; Mills, R.; Thadani, A. N. Terminal Alkynes from Aldehydes via Dehydrohalogenation of (Z)-1-iodo-1-alkenes with TBAF. *Tetrahedron Lett.* **2008**, *49*, 6794–6796.
- (57) Balaraman, K.; Kesavan, V. Efficient Copper(II) acetate Catalyzed Homo- and Heterocoupling of Terminal Alkynes at Ambient Conditions. *Synthesis* **2010**, 3461–3466.
- (58) Shenoy, R. A.; Neubert, M. E.; Abdallah, D. G., Jr.; Keast, S. S.; Petschek, R. G. Synthesis and Mesomorphic Properties of 4-Alkylamino-4'-Substituted Diphenyldiacetylenes. *Liq. Cryst.* **2000**, *27*, 801–812.
- (59) El-Gezawy, H.; Rettig, W.; Lapouyade, R. Model Studies of Spectral and Photophysical Characteristics of Donor-Acceptor-Polyenes: Dimethylamino-Cyano-Diphenylbutadiene. *Chem. Phys. Lett.* **2005**, *401*, 140–148.

(60) Lippert, E. Spectroscopic Determination of the Dipole Moment of Aromatic Compounds in the First Excited Singlet State. *Z. Elektrochem.* **1957**, *61*, 962–975.

(61) Mataga, N.; Kaifu, Y.; Koizumi, M. Solvent Effects Upon Fluorescence Spectra and the Dipole Moments of Excited Molecules. *Bull. Chem. Soc. Jpn.* **1956**, *29*, 465–470.

(62) Lee, C.; Yang, W.; Parr, R. G. Development of the Colle-Salvetti Correlation-Energy Formula into a Functional of the Electron Density. *Phys. Rev. B* **1988**, *37*, 785–789.

(63) Becke, A. D. A New Mixing of Hartree-Fock and Local-Density-Functional Theories. *J. Chem. Phys.* **1993**, *98*, 1372–1377.

(64) Frisch, M. J.; Trucks, G. W.; Schlegel, H. B.; Scuseria, G. E.; Robb, M. A.; Cheeseman, J. R.; Montgomery, Jr., J. A.; Vreven, T.; Kudin, K. N.; Burant, J. C. and et al. *Gaussian 03*, Revision E.01; Gaussian, Inc.: Wallingford, CT, 2004.

(65) Bharathi, S.; Mishra, A. K. Deconvolution of the Fluorescence Spectra into Its Component Gaussians: A Method to Analyze the Binding of Coumarin to Bovine Serum Albumin. *Indian J. Biochem. Biol.* **1999**, *36*, 188–194.

(66) Pitha, J.; Jones, R. N. A Comparison of Optimization Methods for Fitting Curves to Infrared Band Envelopes. *Can. J. Chem.* **1966**, *44*, 3031–3050.

(67) Gans, P.; Gill, J. B. Comments on the Critical Evaluation of Curve Fitting in Infrared Spectrometry. *Anal. Chem.* **1980**, *52*, 351–352.

(68) Bradley, M. S.; Bratu, C. Vibrational Line Profiles as a Probe of Molecular Interactions. *J. Chem. Educ.* **1997**, *74*, 553–555.

(69) Meier, R. J. On Art and Science in Curve-Fitting Vibrational spectra. *Vib. Spectrosc.* **2005**, *39*, 266–269.

(70) Dimmorth, K.; Reichardt, C.; Seipmann, T.; Bohlmann, F. Pyridinium N-Phenolbetaines and Their Use for the Characterization of the Polarity of Solvents. *Justus Liebigs Ann. Chem.* **1963**, *661*, 1–37.

(71) Kosower, E. M.; Tanizawa, K. Analysis of Fluorescence Emission and Quenching for Molecules Bearing Latent Donors. *Chem. Phys. Lett.* **1972**, *16*, 419–425.

(72) Werner, T. C.; Lyon, D. B. Empirical Measures of Solvent Effects on the Fluorescence Energy of Methyl anthroates. *J. Phys. Chem.* **1982**, *86*, 933–939.

(73) Taft, R. W.; Kamlet, M. J. The Solvatochromic Comparison Method 2. The α -Scale of Solvent Hydrogen-Bond Donor (HBD) Acidities. *J. Am. Chem. Soc.* **1976**, *98*, 2886–2894.

(74) Kamlet, M. J.; Abboud, J. L.; Taft, R. W. The Solvatochromic Comparison Method. 6. The π^* Scale of Solvent Polarities. *J. Am. Chem. Soc.* **1977**, *99*, 6027–6038.

(75) Kamlet, M. J.; Taft, R. W. Linear Solvation Energy Relationships. Part 3. Some Reinterpretations of Solvent Effects Based on Correlations with Solvent π^* and α Values. *J. Chem. Soc., Perkin Trans.* **1979**, *2*, 349–356.

(76) Thulstrup, P. W.; Hoffmann, S. V.; Hansen, B. K. V.; Spanget-Larsen, J. Unique Interplay Between Electronic States and Dihedral Angle for the Molecular Rotor Diphenyldiacetylene. *Phys. Chem. Chem. Phys.* **2011**, *13*, 16168–16174.